

Targeting PI3K/mTOR signaling displays potent antitumor efficacy against nonfunctioning pituitary adenomas

Misu Lee¹, Tobias Wiedemann¹, Claudia Gross², Ines Leinhäuser¹, Federico Roncaroli³, Rickmer Braren², Natalia S. Pellegata¹.

Authors affiliations: 1, Institute of Pathology, Helmholtz Zentrum München, Ingolstaedter Landstrasse 1, 85764 Neuheberg, Germany; 2, Institute of Radiology, Klinikum rechts der Isar, Technische Universität München, Munich, Germany; 3, Department of Medicine, Imperial College, London, UK.

Running Title: PI3K/mTOR inhibition in pituitary adenomas.

Key Words: NVP-BEZ235, MENX, pituitary adenomas, preclinical, DW-MRI.

Corresponding author:

Natalia S. Pellegata
Institute of Pathology
Helmholtz Zentrum München,
Ingolstaedter Landstrasse 1
85764 Neuherberg
Germany
Tel.: +49-089-31872633
FAX: +49-089-31873360
e-mail: Natalia.pellegata@helmholtz-muenchen.de

The authors have no conflicts of interest to disclose.

Word count: 5149 (text).

Number of Figures: 6

Abstract

Purpose: Novel therapeutic approaches are needed to improve the postoperative management of residual nonfunctioning pituitary adenomas (NFPAs), given their high relapse rate. Here, we evaluated the antitumor efficacy of the dual PI3K/mTOR inhibitor NVP-BEZ235 in the only available model of spontaneous NFPAs (MENX rats).

Experimental Design: Organotypic cultures of rat primary NFPAs were incubated with NVP-BEZ235 and assessed for cell viability, proliferation, apoptosis, PI3K/mTOR inhibition. NVP-BEZ235, or placebo, was administered to MENX rats and tumor response was monitored non-invasively by diffusion weighted-magnetic resonance imaging (DW-MRI). Following treatment, tumor tissues were investigated for cell proliferation, apoptosis, PI3K/mTOR inhibition. Genes mediating the cytotoxic activity of NVP-BEZ235 were identified by gene expression profiling. Among them, *Defb1*, encoding beta-defensin 1, was further studied for its role in pituitary cells and in human pancreatic neuroendocrine tumor (NET) cells.

Results: NVP-BEZ235 showed anti-proliferative and pro-cell death activities against NFPAs both *in vitro* and *in vivo*, and the response to the drug correlated with inhibition of the PI3K pathway. DW-MRI identified early functional changes (decreased cellularity) in the adenomas before their size was affected and emerged as a useful modality to assess therapy response. The cytotoxic effect of PI3K/mTOR blockade in NFPA was mediated by several genes, including *Defb1*. NVP-BEZ235 treatment induced *Defb1* expression in NFPAs *in vitro* and *in vivo*, and in pancreatic NET cells. High *Defb1* levels sensitized NET cells to PI3K/mTOR inhibition.

Conclusions: Our findings provide rationale for clinical investigation of PI3K/mTOR inhibition in NFPAs and identify novel effectors of PI3K-mediated neuroendocrine cell survival.

Translational Relevance

Nonfunctioning pituitary adenomas (NFPAs) are the second most common type of pituitary adenomas. They are often invasive and not amenable to complete surgical resection. When incompletely removed, their long-term relapse rate is up to 50%. Currently, no effective medical therapy for NFPAs exists. As these tumors show hyperactivation of the PI3K/AKT/mTOR pathway, we tested the efficacy of a dual PI3K/mTOR inhibitor, NVP-BEZ235, in the only spontaneous model of NFPAs (MENX rats), which closely recapitulate human adenomas. Our preclinical *in vitro* and *in vivo* experiments demonstrate cytostatic and cytotoxic action of NVP-BEZ235 in NFPA, and prove the efficacy of targeting PI3K/mTOR in these tumors. Our results may have translational relevance for the medical treatment of patients with residual and recurrent disease. Furthermore, we unveil the molecular readouts of NVP-BEZ235-dependent cell death and identify novel putative therapeutic targets and/or predictors of treatment response in NFPAs and other neuroendocrine tumors.

Introduction

Pituitary adenomas account for 20% of all primary intracranial tumors (1). They can be hormonally active or clinically nonfunctioning. Nonfunctioning pituitary adenomas (NFPAs) represent 30-35% of all pituitary adenomas and about 80% of them are gonadotropinomas (2).

Transsphenoidal surgery is the main-stay treatment of patients with pituitary adenomas. Because of the lack of signs and symptoms secondary to hormone hypersecretion, NFPAs are often diagnosed late when they cause mass effects. At this stage, more than 40% of NFPAs are invasive (3), so that complete surgical removal cannot be achieved. Reported recurrence rate varies between series, with up to 50% of patients experiencing long-term relapse (4, 5). Management of patients with symptomatic residual and recurrent disease is challenging because no medical therapies are currently available. Radiotherapy remains the only post-operative option but it is not curative. Chemotherapy is only used as salvage treatment but usually with disappointing results (6, 7). Therefore, novel therapeutic approaches are required.

Activation of the PI3K/AKT/mTOR pathway plays a pivotal role in the initiation and progression of many human malignancies by enhancing cell survival, stimulating cell proliferation and inhibiting apoptosis (8, 9). Constitutive activation of the PI3K/AKT/mTOR signaling cascade is also a feature of pituitary adenomas and is secondary to mutations or amplification of *PI3KCA* (10, 11) or to overexpression of PI3K (12). NFPAs also display activation of the PI3K/AKT/mTOR pathway (13). Thus, agents inhibiting PI3K signaling might represent an effective therapeutic option for these tumors. In support of this hypothesis, the mTOR inhibitor everolimus was reported to inhibit the viability of primary cultures of human NFPAs *in vitro* (14, 15).

Several compounds have been generated to inhibit the PI3K/AKT/mTOR signaling cascade. The mTOR inhibitor rapamycin and its analogs (rapalogs) are currently used to treat several solid tumors (16, 17). However, the development of drug resistance may limit their efficacy (18). A well-documented mechanism of resistance to rapamycin and rapalogs is the activation of feedback loops on AKT which can re-activate the PI3K pathway (19). To escape the feedback resistance, compounds able to inhibit both mTOR and the upstream PI3K kinase were generated, including NVP-BEZ235, a synthetic small molecule which inhibits both PI3K and mTOR kinase activity by binding to the ATP-binding cleft of these enzymes (20). NVP-BEZ235 has shown potent anti-proliferative activity in preclinical models of

several tumor types (20-24) and is currently evaluated in Phase I/II clinical trials in patients with advanced solid tumors.

MENX is a multitumor syndrome in the rat caused by a biallelic loss-of-function mutation in *Cdkn1b*, encoding the cell cycle inhibitor p27 (25). MENX-affected rats (mutant) develop gonadotroph pituitary adenomas with complete penetrance and represent the only spontaneous model of such tumors. Rat adenomas closely resemble human NFPAs based on histological, immunohistochemical, and ultrastructural data, and are a suitable model for pharmacological studies of pituitary adenomas (26-28).

Purpose of our study was to define the efficacy of PI3K/mTOR inhibition in NFPAs using the MENX rat model of spontaneous gonadotroph pituitary adenomas. We first assessed the effects of NVP-BEZ235 on 3D organotypic cultures of rat primary pituitary adenoma cells *in vitro*. Functional assays suggested that PI3K/mTOR inhibition promotes cytostatic but also cytotoxic effects on pituitary adenoma cells. NVP-BEZ235 was then tested *in vivo* in affected rats. Molecular analyses in combination with functional imaging modalities (diffusion weighted-magnetic resonance imaging, DW-MRI) further pointed to a cytotoxic effect of NVP-BEZ235. DW-MRI emerged as a useful approach for early therapy monitoring of NFPAs following PI3K/mTOR inhibition. Expression array analyses identified the *DEFB1* gene (encoding beta-defensin 1) as a novel mediator of PI3K blockade-dependent cell death and as a potential predictor of therapy response to PI3K inhibitors.

Materials and Methods

Compound preparation

NVP-BEZ235 was kindly supplied by Novartis Pharma. For *in vitro* studies, stock solutions of NVP-BEZ235 were prepared in 100% DMSO and stored at -20°C . Dilutions to the final concentration of $1\mu\text{M}$ were made in the culture medium immediately before use. For *in vivo* experiments, NVP-BEZ235 (45mg/kg, 30 mg/Kg, 20 mg/kg) was suspended in 1 volume of 1-methyl-2-pyrrolidone (Sigma Aldrich) and 9 volumes of PEG300 (Sigma Aldrich).

Organotypic culture

Primary pituitary adenoma cells from mutant rats were isolated as previously reported (26) and organotypic cultures were established using the 3D GravityPLUS™ (InSphero) system. Cells were seeded in a 96-well hanging drop culture platform (GravityPLUSTM, InSphero) in 3D InSight™ Cell Line Maintenance Medium (InSphero) to form spheroids. The spheroids were then transferred to a spheroid-specific 96-well microtissue receiver plate (GravityTRAPT™, InSphero) and further cultivated in the GravityTRAPT™ plates. The spheres were analyzed in an inverted microscope and their size was estimated following treatment using a Hitachi camera HW/C20 installed in a Zeiss Axioplan microscope with Intellicam software (Carl Zeiss MicroImaging GmbH).

Immunostaining

Spheroids and pituitary tumor tissue from MENX rats were collected after 2 weeks of treatment with NVP-BEZ235 or placebo (PEG). They were fixed with 4% paraformaldehyde and embedded in paraffin. Immunohistochemistry (IHC) was performed on an automated immunostainer (Ventana Medical Systems) as previously described (27). Primary antibodies were directed against monoclonal phospho (p)-S6 (S6-S240/244; 1:500; Cell Signaling), monoclonal p-AKT (Ser473; 1:75; Cell Signaling), monoclonal Ki67 (clone B56, 1:100; Dako), monoclonal p27 (1:100; BD Bioscience), polyclonal activated caspase-3 (1:100; Cell signaling), polyclonal α SU (1:1000; supplied by Dr. Parlow, NHPP, UCLA). Antibodies were diluted in Dako REAL™ antibody diluent (Dako). The SuperSensitive IHC detection system from BioGenex was used to visualize the antibody binding following the manufacturer's instructions. Images were recorded using a Hitachi camera HW/C20 (Hitachi) installed in a Zeiss Axioplan microscope with Intellicam software (Carl Zeiss MicroImaging).

For immunofluorescence (IF), we used the primary antibodies used for IHC and the antibody ab115813 against BD-1 (AbCam), and secondary anti-mouse Alexa Fluor® 555 Conjugate (Cell Signaling) or anti-rabbit FITC-conjugated (Invitrogen) antibodies (27). Sections were then analyzed with a Zeiss Axiovert 200 epifluorescence microscope including Apotome unit (Carl Zeiss MicroImaging).

Quantification of P-S6 and cleaved caspase 3 (cc3) staining intensity was performed using Image-J (National Institutes of Health). Images were subjected to the threshold function and we used the same threshold for all images obtained with the same antibody. Then, the percentage of positive area

(P-S6) or the intensity of the staining (cc3) was determined. The Ki67 Labelling Index (LI=percentage of positive nuclei) was estimated as previously reported (28).

Animals and in vivo treatment

This study was approved by the ethics committee on animal research of the government of Upper Bavaria, Germany. MENX-affected rats were maintained as previously reported (29) in agreement with the procedures approved by the Helmholtz Zentrum München, by the Technische Universität München, and by the local government authorities.

Three doses of NVP-BEZ235 were tested in MENX rats: 20, 30 and 45 mg/Kg. As the two higher doses caused a weight loss >10% after 10 days of treatment, the dose of 20mg/Kg was used for further studies. For MRI studies, MENX-affected rats at 7-8 months of age (with sizeable adenomas but still in good general health) were treated for 14 days with NVP-BEZ235 (20 mg/kg) or placebo (PEG) administered daily per oral gavage. The side effect of the drug we observed was mild diarrhea in the last days of the treatment (4/8 rats). Being this our first *in vivo* study of spontaneous rat pituitary adenomas, functional/molecular changes in the tumors were considered more objective and measurable end-points (primary end-points) compared to size and/or survival (secondary end-points).

Pathological analysis

Pituitary tumor tissues of PEG- or NVP-BEZ235-treated rats were fixed in 4% buffered formalin and paraffin-embedded. Three μ m sections were cut and stained with hematoxylin and eosin (H& E), and were evaluated by an experienced neuropathologist (F.R.).

Magnetic resonance imaging

MRI was performed using a 3.0 Tesla clinical MRI system (Ingenia 3.0T, Philips Healthcare, Best, The Netherlands) prior and two weeks after treatment with NVP-BEZ235. Anesthetized animals (2.5 % isoflurane, administered in pure oxygen) were placed in a standard human wrist coil (SENSE Wrist coil 8 elements, Philips Healthcare) in a prone position. T2-weighted (T2w) turbo spin echo (TSE) sequence (slice thickness = 0.7 mm, in plane resolution 0.3x0.3 mm², TR/TE = 3399/106 ms, averages = 12) was performed to assess the tumor volume before and after treatment. Tumor volume was manually segmented and calculated by Osirix (<http://www.osirix-viewer.com>). Statistical analysis (paired t-test) was performed using Prism Graphpad 4 (GraphPad Software, Inc).

Following morphologic T2w imaging, diffusion weighted-MRI (DW-MRI) was performed using a multi-shot spin echo EPI sequence with a total of 6 diffusion weightings: b_{0-5} values = 0, 50, 100, 200, 400 and 600 s/mm², slice thickness 1.4 mm, in plane resolution = 0.62 x 0.78 mm², EPI factor = 7, TR/TE = 4907/62 ms, averages = 2. Three center slices in sagittal orientation, covering the pituitary gland were selected to assess the median apparent diffusion coefficient (ADC) value before and after treatment. Segmented tumors were analyzed by in-house software written in IDL (ITT VIS).

RNA extraction

For RNA extraction from organotypic cultures, spheroids (n=30) were pooled and total RNA was extracted using the automated Maxwell 16 Cell Total RNA Purification Kit with the Maxwell 16 Instrument (Promega). From rat tissues, eight-micrometer sections of freshly prepared pituitary adenomas were stained with toluidine blue using standard manufacturer's protocols with minor modifications. The sections were air-dried and microdissected with a Leica AS LMD Laser Capture Microdissection System using laser pulses of 7.5 μ m diameter, 20-40 mW, and with 2-3 ms duration (Leica). Laser captured tumor tissues were dissolved in 1-Thioglycerol/Homogenization Solution (Promega) and stored at -80°C. RNA extraction was performed as indicated above.

RT2 Profiler™ PCR array and Quantitative TaqMan RT-PCR

For expression array analysis, the first strand cDNA synthesis was performed with the pooled mRNA from organotypic cultures using the RT² First Strand Kit (Qiagen). This cDNA was then added to the RT² SYBR Green qPCR Master Mix (Qiagen) and then each sample was onto the RT² Profiler™ PCR Array Rat Cell Death PathwayFinder (Qiagen). Real-time PCR detection was performed by heating the plate at 95°C for 10 min, followed by 40 cycles of 95°C for 15 s and 60°C for 1 min. Data analysis was performed using the manufacturer's software (<http://www.sabiosciences.com/pcrarraydataanalysis.php>).

Quantitative RT-PCR was performed using TaqMan inventoried primers and probes for the genes indicated in the article and for the rat beta 2-microglobulin gene, mouse beta 2-microglobulin gene or human *TBP* gene as internal controls (Applied Biosystem). The data were analyzed with 2^{- $\Delta\Delta$ Ct} method as previously reported (28).

Cell culture and transfection

The BON1 and QGP1 cell lines were bought from LGC Standards in 2014 and grown as recommended by the manufacturer. The gonadotroph cell line α T3 was a gift of P. Mellon (University of California, San Diego, USA). Since receipt, the cells have not been subsequently authenticated. Cells were grown in DMEM + GlutaMAX™-I (Invitrogen) with 10 % (v/v) FBS (Invitrogen) and 1 % (v/v) penicillin–streptomycin (Invitrogen).

BON1 cells and QGP1 cells were transfected with 20pmol of scrambled (ON TARGETplus Non-targeting siRNA, Dharmacon) or pooled siRNA against human *DEFB1* gene (ON-TARGET plus SMART pool siRNA, Dharmacon) by Amaxa 4D-Nucleofector (Lonza) following the manufacturer's instruction. The target sequences of pooled siRNA against human *DEFB1* gene are: GUUACAGAGGGAAGGCCAA, GCUGUUUACUCUCUGCUUA, GGCCUCAGGUGGUAACUUU and CUGCCCGAUCUUUUACCAA.

Cell proliferation and apoptosis assays

Proliferation of BON1, QGP1 and α T3 cells after treatment was measured with the WST-1 colorimetric assay (Roche) as previously described (30). Cell proliferation in 3D spheroids was measured with the CellTiter-Glo® Cell Viability Assay (Promega) according to the manufacturer's recommendations.

Apoptosis was measured by assessing the activity of caspase-3/7 using Caspase-Glo® 3/7 Assay kit (Promega). BON1 cells and QGP1 cells were transfected with scrambled or anti-DEFB1 siRNA as above, and 24 hrs later treated with NVP-BEZ235 or DMSO for additional 24 hrs. Caspase-3/7 activity was then assessed with a proluminescent caspase-3/7 substrate, which contains the tetrapeptide sequence DEVD. Luminescence was measured with a luminometer (TECAN).

Statistical analysis

Results of the cell assays and Taqman analysis are shown as the mean of values obtained in independent experiments \pm SEM. A paired two-tailed Student's t test was used to detect significance between two series of data, and $P < 0.05$ was considered statistically significant.

Results

PI3K/mTOR inhibition decreases cell proliferation and promotes apoptosis of organotypic 3D cultures of rat primary NFPA cells

Similar to human NFPA (13), MENX-associated pituitary adenomas show activation of the PI3K/AKT/mTOR pathway (26). They therefore represent a suitable experimental model to evaluate novel therapies targeting this signalling cascade.

We previously tested the efficacy of NVP-BEZ235 in primary cultures of dispersed cells from rat adenomas (26). However, cells grown in monolayers are short-lived and do not generally recapitulate the tissue of origin. For this reason, we here established 3D organotypic cultures of rat primary adenoma cells and documented that in 2-week-old cultures the expression of the common alpha subunit (α SU), of phosphorylated (P)-S6 (S6-S240/244), a downstream target of mTOR, and the Ki67 labelling index (LI) were similar to the primary tumors of origin (Supplementary Fig. S1) (27).

Organotypic cultures from three mutant rats (96 spheres each) were treated for two weeks with NVP-BEZ235 or DMSO. The surface area of 10 spheroids per culture was measured at the beginning and at the end of the treatment to assess their growth. A statistically significant reduction in size (-33%; $P < 0.001$ versus DMSO control) (Fig. 1A) and a decrease in cell viability (-43%; $P < 0.01$ versus DMSO control) (Fig 1B) were observed in the spheroids treated with NVP-BEZ235 but not in those incubated with DMSO. Drug-treated 3D cultures showed both a dramatic decrease in P-S6 and reduced cell proliferation, as assessed by Ki67 staining (Fig. 1C). Treatment of organotypic cultures with NVP-BEZ235 also induced the activation of caspase-3 (cleaved caspase 3, cc3) while no increase was seen in spheres treated with DMSO (Fig. 1C). These experiments confirmed the inhibition of the PI3K/AKT/mTOR pathway by NVP-BEZ235 and its anti-proliferative and pro-cell death effects *in vitro* on NFPA cells.

PI3K/mTOR inhibition reduces cell proliferation and promotes cell death in a model of endogenous NFPA in vivo

To understand the effect of NVP-BEZ235 in spontaneous pituitary adenomas, we treated MENX rats with the drug. We first verified whether the drug reached the pituitary and repressed the PI3K pathway, as shown *in vitro*. NVP-BEZ235 (45mg/kg) or PEG (placebo) was administered to MENX rats (n=2 each group) by oral gavage and animals were sacrificed 1hr or 6hrs post-treatment. Immunostains for P-AKT and P-S6 showed considerable reduction of the two proteins, and

particularly of P-S6, 6hrs after administration of NVP-BEZ235 when compared with PEG-treated rats (Supplementary Fig. S2A). In contrast, decrease in P-AKT and P-S6 was not significant at 1hr post-treatment (Supplementary Fig. S2A). The same tissues were also analyzed by Imaging Mass Spectrometry (MALDI Imaging). At 6hrs post-treatment, but not at 1h post-treatment, the pituitary adenomas of NVP-BEZ235-treated rats had a proteomic profile significantly different from the tumors of placebo-treated rats (Supplementary Fig. S2B), thereby providing indirect evidence that the drug had reached the pituitary.

These results led us to treat mutant rats for two weeks with 20 mg/kg NVP-BEZ235 or PEG (placebo) both administered daily per oral gavage (Fig. 2A). At the end of the treatment, *ex vivo* tissue analysis showed that P-S6 expression and Ki67 labeling index (LI) were reduced in drug-treated pituitary adenomas and that cleaved caspase-3 (cc3) was increased (Fig. 2B) indicating efficacy of NVP-BEZ235 to inhibit PI3K/mTOR and to elicit multifaceted antitumor activities in NFPAs *in vivo*. Quantification of the P-S6 and cc3 stainings and assessment of the Ki67 LI in the tumor tissues are shown in Figure 2D-E.

Pathological examination of NVP-BEZ235-treated adenomas (20mg/Kg) showed pronounced vacuolation of the cytoplasm when compared to PEG-treated animals (Supplementary Fig. S3). Vacuoles appeared even more prominent at the 30mg/Kg and 45mg/Kg doses (Supplementary Fig. S3 and data not shown). All treated tumors contained macrophages in variable number but none of them showed overt necrosis.

Diffusion weighted MRI shows a reduction in cellularity in NVP-BEZ235-treated rats

We then asked the question as to whether we can monitor the response to NVP-BEZ235 non-invasively in living MENX rats. Diffusion weighted magnetic resonance imaging (DW-MRI) with calculated mean apparent diffusion coefficient (ADC) values were used to assess changes in tumor cellularity (31) as indication of response to therapy. ADC values were obtained for all mutant rats (n=12) at day 0 (pre-therapy scans), and then 14 days after daily administration of 20mg/kg NVP-BEZ235 to a subset of animals (n=8), or of placebo (PEG) to the remaining ones (n=4) (post-therapy scans). Three sagittal center slices were used to calculate a mean ADC for each pituitary gland. As shown in Fig. 3, we observed significantly increased ADC values after NVP-BEZ235 treatment (mean ADC pre=0,6325 *versus* mean ADC post=0,8146; $p = 0.0013$) while no significant changes were

observed in placebo-treated rats (mean ADC pre = 0,7059 *versus* mean ADC post = 0,7058; p = 0.999).

In parallel to the DW-MRI, we measured volumetric changes of the pituitary tumors before and after treatment with NVP-BEZ235 or with PEG by conventional T2w MRI. A slight decrease in tumor size was observed in NVP-BEZ235-treated animals (mean tumor volume pre = 0,0359 cm³ *versus* mean tumor volume post = 0,0348 cm³), albeit it did not reach the statistical significance by paired t-test (Fig 3B). Conversely, a slight increase in tumor size was observed in placebo-treated rats (mean tumor volume pre = 0,0355 cm³ *versus* mean tumor volume post = 0,0399 cm³). Probably a 14-day course of treatment is not long enough to elicit tumor shrinkage to an extent detectable by neuroimaging.

Thus, DW-MRI, assessing a functional parameter such as the induction of cell death, might be useful for early response tumor monitoring following PI3K/mTOR inhibition in pituitary adenomas before changes in tumor volume take place.

Gene expression array analysis of NVP-BEZ235-treated 3D pituitary adenoma cultures identifies novel targets of the PI3K pathway

We then explored the molecular mechanisms mediating NVP-BEZ235-induced cell death in NFPAs. We performed gene expression profiling of organotypic cultures derived from five independent rat pituitary adenomas following 2 weeks of treatment with NVP-BEZ235 or with DMSO. Genetic signatures were obtained using PCR-based arrays containing 84 cell death-related genes. By employing a >1.5 fold-change cut-off for gene expression changes, a total of 26 genes were found to be differentially expressed between the two groups. Twelve genes were up-regulated in drug-treated *versus* placebo-treated cells, and 14 genes were down-regulated (Supplementary Fig. S4). Based on their functional annotation eleven including *Foxi1*, *Defb1* and *Tnfrsf8* were involved in necrosis. Seven genes, including *Tnfrsf10b*, *Cd40lg*, *Bcl2a1* were related to apoptosis and the remaining ones play a role in autophagy.

Next, we verified whether three of the genes found to be downstream of the PI3K/AKT/mTOR pathway in pituitary adenomas cells *in vitro* (i.e. *Defb1* and *Tnfrsf10b* up-regulated, *Bcl2a1* down-regulated) are targets of this signaling cascade also *in vivo*. MENX mutant rats were treated with NVP-BEZ235 (n=4) or placebo (PEG; n=4) for 2 weeks, and then the expression of these 3 genes was assessed in their pituitary glands by quantitative (q)RT-PCR analyses. As shown in Fig 4, *Defb1* and *Tnfrsf10b* were up-regulated by a +7.68 and +2.62 fold change (P<0.05), respectively, in the

tumors of NVP-BEZ235-treated rats when compared with tumors of placebo-treated animals. The anti-apoptotic gene *Bcl2a1* was down-regulated in pituitary tumors after NVP-BEZ235 treatment (-0.5 fold change *versus* placebo; $P < 0.05$) (Fig. 4). These *in vivo* data are consistent with those obtained analyzing pituitary adenoma organotypic cultures *in vitro*.

In conclusion, gene expression array analysis identified novel genes mediating the cytotoxic effect of PI3K/mTOR inhibition in NFPAs.

Defb1 is a target of PI3K/mTOR inhibition in pituitary adenomas and in other neuroendocrine tumor (NET) cells

Among the cell death-related genes induced by PI3K/mTOR inhibition in rat NFPAs, *Defb1* is particularly interesting. This gene encodes beta-defensin 1 (BD-1), a member of a highly conserved group of host defence peptide (32). Defensins play an important role in processes other than innate immunity (33). In human cancers, BD-1 has been proposed to act as a tumor suppressor as it inhibits cell growth and promotes apoptosis (34-37). Currently, the extent of expression and role of *DEFB1* in NETs, and in pituitary adenomas in particular, is unknown.

For this reason, we determined the level of expression of *DEFB1* in human NFPAs (n=6) by qRT-PCR and compared it with normal human pituitary tissues (n=3). The results showed that *DEFB1* is extremely down-regulated in human NFPAs when compared with normal pituitary (Fig. 5A). We also checked the expression of the BD-1 protein in human clinically nonfunctioning gonadotroph adenomas (n=10) by immunofluorescence. Only one out of 10 tumors showed weak expression while the others were negative (Fig. 5B). In the normal human anterior pituitary, BD-1 was expressed and was found to colocalise with luteinizing hormone (LH) (Supplementary Fig. S5), indicating that BD-1 is expressed in normal gonadotroph cells and suggesting that BD-1 is lost in gonadotroph adenomas.

Next, we investigated the role of *DEFB1* in NFPA by performing functional *in vitro* studies. Currently there are no established human/rodent NFPA/gonadotroph adenoma cell lines, so we tested α T3, a mouse immortalized gonadotroph cell line (38). Similar to the rat primary adenoma cells, also α T3 cells showed an increase in beta-defensin 1 expression at both the mRNA and protein level (by immunofluorescence) upon NVP-BEZ235 treatment (Fig. 5C and D). Concomitantly, a reduction in the levels of both P-AKT and P-S6 was observed in response to drug treatment (Fig. 5E), confirming the inhibition of PI3K/mTOR signaling in α T3 cells.

To verify whether BD-1 plays a more general role in NETs, we also analysed two well-characterized cell lines, BON1 and QGP1, both derived from human pancreatic endocrine tumors. Both cell lines express *DEFB1* (Fig. 6C). Similar to rat primary pituitary adenoma cells and mouse gonadotroph cells, also treatment of BON1 and QGP1 with NVP-BEZ235 induced the levels of both *DEFB1* mRNA and BD-1 protein (Fig. 6A-C). In agreement with previously published data (39), we observed that incubation with NVP-BEZ235 decreased the proliferation and increased the apoptosis of both cell lines, this latter assessed by measuring caspase 3/7 activity (Fig. 6D-G).

We then wondered whether the induction of *DEFB1* sensitizes NET cells to PI3K/mTOR inhibition. Thus, we silenced *DEFB1* expression by siRNA-mediated gene knockdown in BON1 and QGP1 cells and we then treated them with NVP-BEZ235. We could demonstrate that the knockdown of *DEFB1* by specific si-*DEFB1* molecules reduces the antitumor effect of the drug. Indeed, there was a more prominent decrease in cell proliferation (Fig. 6D and F) and increase in apoptosis (caspase 3/7 activity) in cells transfected with unspecific scrambled siRNA than in cells transfected with si-*DEFB1* (Fig. 6E and G). Efficient *DEFB1* gene silencing was confirmed by qRT-PCR (Supplementary Fig. S6).

Altogether, these data suggest that *DEFB1* is a downstream target of the PI3KmTOR pathway in human NETs, where it mediates pro-apoptotic signals, and is a putative predictor of therapy response.

Discussion

We have previously shown that NVP-BEZ235 can potently inhibit cell proliferation of both dispersed rat primary pituitary adenoma cells and established adenoma cell lines *in vitro* (26). Here, we expanded these studies to include organotypic cultures of rat primary pituitary tumors, better models of the situation in tissues. We demonstrated that drug treatment induces potent anti-proliferative and pro-apoptotic effects in NFPAs. Moreover, we have established the utility of NVP-BEZ235 as a cytotoxic agent in a preclinical *in vivo* model of spontaneous NFPAs. In our tumor model, the *in vitro* sensitivity of NFPAs to NVP-BEZ235 corresponds to the *in vivo* sensitivity and both correlate with inhibition of downstream effectors of the PI3K pathway. To date, NVP-BEZ235 has been shown to behave as a cytostatic or cytotoxic antitumor agent, depending on the tumor type. In NFPAs, this compound

displays both activities. Similarly, Dai et al. (40) reported that the PI3K/mTOR inhibitor XL765, alone or in combination with temozolomide (TMZ), inhibits proliferation and induces caspase-3/7 activity in a xenograft model of pituitary somatotroph adenoma cells (GH3 cells). In our animal model, NVP-BEZ235 can reduce the proliferation and induce apoptosis of the pituitary adenomas in their natural anatomical location.

For many solid tumors it typically takes several months to evaluate therapy response based on RECIST criteria (41) when using solely morphological imaging methods with soft tissue contrast (e.g. CT or MRI). Thus, the identification of parameters that could be used as surrogate markers of response to therapy is of pivotal importance. Their assessment by functional imaging modalities could help to quickly identify non-responders, thus minimizing potential side effects (and costs) by early discontinuation of an ineffective therapy. In our study, we showed that non-invasive DW-MRI is a useful imaging modality for the early therapy response monitoring of NFPAs treated with a PI3K/mTOR inhibitor. DW imaging can characterize tumor physiology and morphology and provide information about cellular consistency, which reflects in lower or higher ADC values. Indeed, NVP-BEZ235 administration *in vivo* resulted in a significant increase in ADC values, mirroring reduced cellular density and enhanced cell death, after only 2 weeks of treatment, whereas no changes in ADC values were detected in rats treated with placebo only. Importantly, changes in ADC values following drug treatment preceded significant changes in pituitary tumor volume, as measured by anatomical MRI. Recent studies performed in other tumor entities including gastrointestinal stromal tumors, hepatocellular carcinomas and breast cancer propose DW-MRI as a surrogate marker of response to chemotherapy (42-44). As shown in a xenograft model of prostate cancer, changes in water molecule diffusion and ADC values can be detected already 24 hrs after photodynamic therapy (45). Based on our data, DW-MRI has great potential as an imaging biomarker for early prediction of the response of NFPAs to PI3K/mTOR inhibition.

In an attempt to identify the genes mediating the cytotoxic role of PI3K inhibition in our model, we performed gene expression analyses of organotypic cultures treated with NVP-BEZ235, or placebo-treated, focusing on cell death-related genes. Several genes were found differentially expressed between the two sample groups, supporting the hypothesis of an important role of active PI3K signaling in pituitary adenoma cell survival. *Defb1*, encoding BD-1, was among the genes significantly up-regulated following NVP-BEZ235 treatment (but not placebo treatment), and was never so far studied in the context of pituitary adenomas. Besides its role as the most important

antimicrobial peptide in epithelial tissues, BD-1 was recently found to be involved in a variety of processes other than innate immunity, including immunomodulation, development, wound healing and cancer (33). In human cancers, BD-1 has been proposed to act as a tumor suppressor in renal clear cell carcinoma and prostate cancer since its expression is lower in the tumors compared with preneoplastic or normal tissues, and its ectopic overexpression induces caspase-3-mediated apoptosis (35, 37). The mechanism of down-regulation of *DEFB1* in the above tumors has not been fully elucidated, but methylation does not seem to play an important role (37). Consistent with these studies, we found that both *DEFB1* and BD-1 are virtually not expressed in human NFPAs, suggesting that *DEFB1* might represent a novel tumor suppressor gene in NFPAs.

In contrast to the adenomas, BD-1 is expressed in gonadotroph cells of the normal pituitary gland. BD-1 is generally expressed in epithelial cells of the gastrointestinal and broncho-respiratory tract, tissues involved in host defence, and only one study so far has reported BD-1 expression in the posterior lobe of the pituitary (neurohypophysis) of the fish orange-spotted grouper, where it plays a still unidentified role (46).

We here show, for the first time, that BD-1 expression modulates the response to antitumor drugs. Indeed, we demonstrate that, concomitantly with promoting antitumor activities, PI3K/mTOR blockade up-regulates *Defb1/DEFB1* in various neuroendocrine cell models (pituitary and pancreatic) *in vitro*, as well as in MENX-associated pituitary adenomas *in vivo*. Silencing of the *DEFB1* gene in human BON1 and QGP1 cells abolished in part the anti-proliferative and pro-apoptotic effect of NVP-BEZ235, suggesting that *DEFB1* is among the factors mediating the cytostatic and cytotoxic effect of the drug. Based on these findings, we propose that the increase in *DEFB1* expression upon treatment with PI3K/mTOR inhibitors sensitizes human NET cells, and possibly NFPAs, to these compounds.

Renal clear cell carcinoma, prostate cancer, as well as NFPAs, are characterized by hyperactivation of the PI3K pathway (12, 47, 48) and concomitantly were found not to express *DEFB1* (35, 37 and this study). It is tempting to speculate that the down-regulation of *DEFB1* in these tumors might be mediated by activation of the PI3K/AKT/mTOR pathway, possibly through modulation of transcription factors activity. Consistent with this hypothesis, we observed that pharmacologic blockade of PI3K signaling rescues *DEFB1* expression in NFPAs and NET cells. Currently, there are no data directly connecting the PI3K pathway and the transcriptional regulation of the *DEFB1* gene. It has been reported that *DEFB1* expression is repressed by the transcription factor PAX2 in prostate cancer cells (49). Inhibition of PI3K activity leads to a downregulation of PAX2 expression in renal tubular cells

(50). PAX2 is expressed in the endocrine pancreas (from which BON1 and QGP1 cells derive) (51) but no information on the pituitary gland is available. Thus, we could envision a mechanism whereby inhibition of PI3K signalling in NET cells decreases PAX2 expression which in turn up-regulates *DEFB1*. Further studies are required to verify this hypothesis.

Bcl2a1/Bfl-1 was also among the genes differentially expressed in NVP-BEZ235-treated *versus* placebo-treated primary pituitary adenoma cells. In contrast to *Defb1*, its expression was reduced by the drug treatment *in vitro* and *in vivo*. Bfl-1 is an anti-apoptotic member of the Bcl-2 family of cell death regulators. In a physiological context, Bfl-1 is mainly expressed in the hematopoietic system, where it facilitates the survival of selected leukocytes subsets. *Bfl-1* has been found overexpressed in a subset of chemoresistant tumors, where it protects tumor cells from chemotherapy-induced apoptosis (52). Recently, peptide aptamers specifically targeting Bfl-1 have been generated and shown to sensitize B-cell lymphoma cell lines to chemotherapeutic drugs through induction of apoptosis (53, 54). Given that NFPAs are usually resistant to traditional cytotoxic chemotherapeutic agents (2, 6), down-regulation of *Bfl1* by NVP-BEZ235 might represent a useful strategy to sensitize these tumors to apoptosis induced by conventional chemotherapy.

Altogether, our gene expression studies unveiled novel putative targets in NFPAs that deserve to be further evaluated for their therapeutic potential.

Of the several inhibitors of the PI3K signaling cascade, only everolimus (a mTOR inhibitor) has been so far evaluated in one patient with an aggressive pituitary tumor, specifically, with an ACTH-secreting pituitary carcinoma (55). Everolimus was ineffective at normalizing hormone secretion and at controlling tumor growth. The lack of efficacy of everolimus could be ascribed to the well-documented feedback loop of rapalogs on AKT phosphorylation, already extensively associated with drug resistance in a variety of human cancers (18). To overcome tumor cell resistance to these drugs, dual inhibitors have been developed that block mTOR but also the upstream PI3K kinase, such as NVP-BEZ235. Here we demonstrate that dual PI3K/mTOR inhibition is highly effective against NFPAs *in vitro* and *in vivo*. These preclinical trials performed on an endogenous model of NFPAs provide the rationale for targeting PI3K/mTOR signaling in patients with pituitary adenomas, especially those with large and invasive NFPAs at high risk for tumor relapse.

Disclosure of Potential Conflicts of Interest

No potential conflicts of interest were disclosed.

Authors' Contributions

Conception and design: M. Lee, N.S. Pellegata

Development of methodology: M. Lee, T. Wiedemann, N.S. Pellegata

Acquisition of data: M. Lee, T. Wiedemann, C. Gross, R. Braren, N.S. Pellegata

Analysis and interpretation of data: M. Lee, C. Gross, F. Roncaroli, R. Braren, N.S. Pellegata

Writing, review, and/or revision of the manuscript: M. Lee, F. Roncaroli, R. Braren, N.S. Pellegata

Study supervision: N.S. Pellegata

Grant Support

N.S. Pellegata is supported by grants SFB824, subproject B08, from the Deutsche Forschungsgemeinschaft (DFG) and grant #110874 from the Deutsche Krebshilfe, and also in part by a research grant from Novartis Pharma GmbH, Nürnberg, Germany.

Acknowledgements

We thank E. Samson and E. Pulz for excellent technical assistance and Novartis for providing us with NVP-BEZ235. We are grateful to the Imperial College Healthcare NHS Trust Tissue Bank for supplying human gonadotroph adenomas and to the UK Parkinson's Disease and Multiple Sclerosis Tissue Bank for supplying normal human pituitary tissues.

References

1. Pereira AM, Biermasz NR. Treatment of nonfunctioning pituitary adenomas: what were the contributions of the last 10 years? A critical view. *Ann Endocrinol (Paris)*. 2012;73:111-6.
2. Greenman Y, Stern N. Non-functioning pituitary adenomas. *Best practice & research Clinical endocrinology & metabolism*. 2009;23:625-38.
3. Brochier S, Galland F, Kujas M, Parker F, Gaillard S, Raftopoulos C, et al. Factors predicting relapse of nonfunctioning pituitary macroadenomas after neurosurgery: a study of 142 patients. *European journal of endocrinology / European Federation of Endocrine Societies*. 2010;163:193-200.
4. Losa M, Donofrio CA, Barzaghi R, Mortini P. Presentation and surgical results of incidentally discovered nonfunctioning pituitary adenomas: evidence for a better outcome independently of other patients' characteristics. *Eur J Endocrinol*. 2013;169:735-42.
5. Berkman S, Schlaffer S, Nimsky C, Fahlbusch R, Buchfelder M. Follow-up and long-term outcome of nonfunctioning pituitary adenoma operated by transsphenoidal surgery with intraoperative high-field magnetic resonance imaging. *Acta Neurochir* 2014;156:2233-43.
6. Colao A, Filippella M, Pivonello R, Di Somma C, Faggiano A, Lombardi G. Combined therapy of somatostatin analogues and dopamine agonists in the treatment of pituitary tumours. *European journal of endocrinology / European Federation of Endocrine Societies*. 2007;156 Suppl 1:S57-63.
7. Greenman Y, Tordjman K, Osher E, Veshchev I, Shenkerman G, Reider G, II, et al. Postoperative treatment of clinically nonfunctioning pituitary adenomas with dopamine agonists decreases tumour remnant growth. *Clin Endocrinol (Oxf)*. 2005;63:39-44.
8. Cantrell DA. Phosphoinositide 3-kinase signalling pathways. *J Cell Sci*. 2001;114:1439-45.
9. Hennessy BT, Smith DL, Ram PT, Lu Y, Mills GB. Exploiting the PI3K/AKT pathway for cancer drug discovery. *Nat Rev Drug Discov*. 2005;4:988-1004.
10. Lin Y, Jiang X, Shen Y, Li M, Ma H, Xing M, et al. Frequent mutations and amplifications of the PIK3CA gene in pituitary tumors. *Endocrine-related cancer*. 2009;16:301-10.
11. Murat CB, Braga PB, Fortes MA, Bronstein MD, Correa-Giannella ML, Giorgi RR. Mutation and genomic amplification of the PIK3CA proto-oncogene in pituitary adenomas. *Braz J Med Biol Res*. 2012;45:851-5.
12. Cakir M, Grossman AB. Targeting MAPK (Ras/ERK) and PI3K/Akt pathways in pituitary tumorigenesis. *Expert Opin Ther Targets*. 2009;13:1121-34.
13. Monsalves E, Juraschka K, Tateno T, Agnihotri S, Asa SL, Ezzat S, Zadeh G. The PI3K/AKT/mTOR pathway in the pathophysiology and treatment of pituitary adenomas. *Endocr Relat Cancer*. 2014;21:R331-44.
14. Cerovac V, Monteserin-Garcia J, Rubinfeld H, Buchfelder M, Losa M, Florio T, et al. The somatostatin analogue octreotide confers sensitivity to rapamycin treatment on pituitary tumor cells. *Cancer research*. 2010;70:666-74.
15. Zatelli MC, Minoia M, Filieri C, Tagliati F, Buratto M, Ambrosio MR, et al. Effect of everolimus on cell viability in nonfunctioning pituitary adenomas. *J Clin Endocrinol Metab*. 2010;95:968-76.
16. Majumder PK, Febbo PG, Bikoff R, Berger R, Xue Q, McMahon LM, et al. mTOR inhibition reverses Akt-dependent prostate intraepithelial neoplasia through regulation of apoptotic and HIF-1-dependent pathways. *Nat Med*. 2004;10:594-601.

17. Neshat MS, Mellinshoff IK, Tran C, Stiles B, Thomas G, Petersen R, et al. Enhanced sensitivity of PTEN-deficient tumors to inhibition of FRAP/mTOR. *Proc Natl Acad Sci U S A*. 2001;98:10314-9.
18. Huang S, Houghton PJ. Resistance to rapamycin: a novel anticancer drug. *Cancer metastasis reviews*. 2001;20:69-78.
19. O'Reilly KE, Rojo F, She QB, Solit D, Mills GB, Smith D, et al. mTOR inhibition induces upstream receptor tyrosine kinase signaling and activates Akt. *Cancer research*. 2006;66:1500-8.
20. Maira SM, Stauffer F, Brueggen J, Furet P, Schnell C, Fritsch C, et al. Identification and characterization of NVP-BEZ235, a new orally available dual phosphatidylinositol 3-kinase/mammalian target of rapamycin inhibitor with potent in vivo antitumor activity. *Mol Cancer Ther*. 2008;7:1851-63.
21. Baumann P, Mandl-Weber S, Oduncu F, Schmidmaier R. The novel orally bioavailable inhibitor of phosphoinositol-3-kinase and mammalian target of rapamycin, NVP-BEZ235, inhibits growth and proliferation in multiple myeloma. *Exp Cell Res*. 2009;315:485-97.
22. Serra V, Markman B, Scaltriti M, Eichhorn PJ, Valero V, Guzman M, et al. NVP-BEZ235, a dual PI3K/mTOR inhibitor, prevents PI3K signaling and inhibits the growth of cancer cells with activating PI3K mutations. *Cancer Res*. 2008;68:8022-30.
23. Schnell CR, Stauffer F, Allegrini PR, O'Reilly T, McSheehy PM, Dartois C, et al. Effects of the dual phosphatidylinositol 3-kinase/mammalian target of rapamycin inhibitor NVP-BEZ235 on the tumor vasculature: implications for clinical imaging. *Cancer Res*. 2008;68:6598-607.
24. Cao P, Maira SM, Garcia-Echeverria C, Hedley DW. Activity of a novel, dual PI3-kinase/mTOR inhibitor NVP-BEZ235 against primary human pancreatic cancers grown as orthotopic xenografts. *Br J Cancer*. 2009;100:1267-76.
25. Pellegata NS. MENX and MEN4. *Clinics*. 2012;67 Suppl 1:13-8.
26. Lee M, Theodoropoulou M, Graw J, Roncaroli F, Zatelli MC, Pellegata NS. Levels of p27 sensitize to dual PI3K/mTOR inhibition. *Mol Cancer Ther*. 2011;10:1450-9.
27. Marinoni I, Lee M, Mountford S, Perren A, Bravi I, Jennen L, et al. Characterization of MENX-associated pituitary tumours. *Neuropathol Appl Neurobiol*. 2013;39:256-69.
28. Lee M, Marinoni I, Irmeler M, Psaras T, Honegger JB, Beschorner R, et al. Transcriptome analysis of MENX-associated rat pituitary adenomas identifies novel molecular mechanisms involved in the pathogenesis of human pituitary gonadotroph adenomas. *Acta Neuropathol*. 2013;126:137-50.
29. Fritz A, Walch A, Piotrowska K, Rosemann M, Schaffer E, Weber K, et al. Recessive transmission of a multiple endocrine neoplasia syndrome in the rat. *Cancer research*. 2002;62:3048-51.
30. Lee M, Waser B, Reubi JC, Pellegata NS. Secretin receptor promotes the proliferation of endocrine tumor cells via the PI3K/AKT pathway. *Mol Endocrinol*. 2012;26:1394-405.
31. Thoeny HC, Ross BD. Predicting and monitoring cancer treatment response with diffusion-weighted MRI. *Journal of magnetic resonance imaging : JMRI*. 2010;32:2-16.
32. Valore EV, Park CH, Quayle AJ, Wiles KR, McCray PB, Jr., Ganz T. Human beta-defensin-1: an antimicrobial peptide of urogenital tissues. *J Clin Invest*. 1998;101:1633-42.
33. Mansour SC, Pena OM, Hancock RE. Host defense peptides: front-line immunomodulators. *Trends Immunol*. 2014;35:443-50.
34. Han Q, Wang R, Sun C, Jin X, Liu D, Zhao X, et al. Human beta-defensin-1 suppresses tumor migration and invasion and is an independent predictor for survival of oral squamous cell carcinoma patients. *PLoS One*. 2014;9:e91867.
35. Donald CD, Sun CQ, Lim SD, Macoska J, Cohen C, Amin MB, et al. Cancer-specific loss of beta-defensin 1 in renal and prostatic carcinomas. *Lab Invest*. 2003;83:501-5.

36. Gambichler T, Skrygan M, Huyn J, Bechara FG, Sand M, Altmeyer P, et al. Pattern of mRNA expression of beta-defensins in basal cell carcinoma. *BMC Cancer*. 2006;6:163.
37. Sun CQ, Arnold R, Fernandez-Golarz C, Parrish AB, Almekinder T, He J, et al. Human beta-defensin-1, a potential chromosome 8p tumor suppressor: control of transcription and induction of apoptosis in renal cell carcinoma. *Cancer research*. 2006;66:8542-9.
38. Windle JJ, Weiner RI, Mellon PL. Cell lines of the pituitary gonadotrope lineage derived by targeted oncogenesis in transgenic mice. *Mol Endocrinol*. 1990;4:597-603.
39. Valentino JD, Li J, Zaytseva YY, Mustain WC, Elliott VA, Kim JT, et al. Cotargeting the PI3K and RAS pathways for the treatment of neuroendocrine tumors. *Clinical cancer research : an official journal of the American Association for Cancer Research*. 2014;20:1212-22.
40. Dai C, Zhang B, Liu X, Ma S, Yang Y, Yao Y, et al. Inhibition of PI3K/AKT/mTOR pathway enhances temozolomide-induced cytotoxicity in pituitary adenoma cell lines in vitro and xenografted pituitary adenoma in female nude mice. *Endocrinology*. 2013;154:1247-59.
41. Eisenhauer EA, Therasse P, Bogaerts J, Schwartz LH, Sargent D, Ford R, et al. New response evaluation criteria in solid tumours: revised RECIST guideline (version 1.1). *European journal of cancer*. 2009;45:228-47.
42. Iwasa H, Kubota K, Hamada N, Nogami M, Nishioka A. Early prediction of response to neoadjuvant chemotherapy in patients with breast cancer using diffusion-weighted imaging and gray-scale ultrasonography. *Oncol Rep*. 2014;31:1555-60.
43. Schmidt S, Dunet V, Koehli M, Montemurro M, Meuli R, Prior JO. Diffusion-weighted magnetic resonance imaging in metastatic gastrointestinal stromal tumor (GIST): a pilot study on the assessment of treatment response in comparison with 18F-FDG PET/CT. *Acta Radiol*. 2013;54:837-42.
44. Lim KS. Diffusion-weighted MRI of hepatocellular carcinoma in cirrhosis. *Clin Radiol*. 2014;69:1-10.
45. Wang H, Fei B. Diffusion-weighted MRI for monitoring tumor response to photodynamic therapy. *Journal of magnetic resonance imaging : JMRI*. 2010;32:409-17.
46. Jin JY, Zhou L, Wang Y, Li Z, Zhao JG, Zhang QY, et al. Antibacterial and antiviral roles of a fish beta-defensin expressed both in pituitary and testis. *PLoS One*. 2010;5:e12883.
47. Sourbier C, Lindner V, Lang H, Agouni A, Schordan E, Danilin S, et al. The phosphoinositide 3-kinase/Akt pathway: a new target in human renal cell carcinoma therapy. *Cancer research*. 2006;66:5130-42.
48. Sarker D, Reid AH, Yap TA, de Bono JS. Targeting the PI3K/AKT pathway for the treatment of prostate cancer. *Clinical cancer research : an official journal of the American Association for Cancer Research*. 2009;15:4799-805.
49. Bose SK, Gibson W, Bullard RS, Donald CD. PAX2 oncogene negatively regulates the expression of the host defense peptide human beta defensin-1 in prostate cancer. *Mol Immunol*. 2009;46:1140-8.
50. Shen W, Brown NS, Finn PF, Dice JF, Franch HA. Akt and Mammalian target of rapamycin regulate separate systems of proteolysis in renal tubular cells. *J Am Soc Nephrol*. 2006;17:2414-23.
51. Ritz-Laser B, Estreicher A, Gauthier B, Philippe J. The paired homeodomain transcription factor Pax-2 is expressed in the endocrine pancreas and transactivates the glucagon gene promoter. *J Biol Chem*. 2000;275:32708-15.
52. Ck H, Mj C, Cl H, C C, S J, Ms C. The Role of the Pro-Survival Molecule Bfl-1 in Melanoma. *Int J Biochem Cell Biol*. 2014.
53. Brien G, Trescol-Biemont MC, Bonnefoy-Berard N. Downregulation of Bfl-1 protein expression sensitizes malignant B cells to apoptosis. *Oncogene*. 2007;26:5828-32.

54. Brien G, Debaud AL, Bickle M, Trescol-Biemont MC, Moncorge O, Colas P, et al. Characterization of peptide aptamers targeting Bfl-1 anti-apoptotic protein. *Biochemistry*. 2011;50:5120-9.
55. Jouanneau E, Wierinckx A, Ducray F, Favrel V, Borson-Chazot F, Honnorat J, et al. New targeted therapies in pituitary carcinoma resistant to temozolomide. *Pituitary*. 2012;15:37-43.

Figure legends

Fig 1. Effect of the dual PI3K/mTOR inhibitor NVP-BEZ235 on 3D organotypic cultures of rat primary NFPA cells. (A) 3D cultures obtained from rat primary pituitary adenomas were treated daily with 1 μ M NVP-BEZ235 or DMSO for 14 days. Then, representative spheres were analyzed in an inverted microscope and their size was estimated using the Image-Pro Analyzer software. Data were analyzed independently with 10 replicates each culture and are expressed as the mean \pm SEM. (B) In parallel, cell viability of the 3D cultures was assessed by measuring ATP levels using the CellTiter-Glo[®] Luminescent Cell Viability Assay. Data were analyzed independently with 6 replicates each culture and are expressed as the mean \pm SEM. **, P < 0.01; ***, P < 0.001 *versus* DMSO. (C) Phase contrast images of selected spheres following 14 days of DMSO or 1 μ M NVP-BEZ235 treatment (upper panels). After treatment, 3D cultures were embedded in paraffin and indirect immunofluorescence was performed using antibodies against pS6 (Ser240/244), Ki67, or cleaved caspase-3 (cc3). Scale bars: 200 μ m (upper panels), 50 μ m (immunofluorescence).

Fig 2. Effect of the dual PI3K/mTOR inhibitor NVP-BEZ235 *in vivo*. (A) Scheme of the treatment course. Affected rats were scanned using DW-MRI on Day 0 and then on Day 2 treatment with either 20mg/Kg of NVP-BEZ235 (n=8) or placebo (n=4) was started and continued for 14 days. Rats were again subjected to DW-MRI on day 17 and then necropsy was performed and tissues collected. (B) Pituitary tumors were collected after 14 days of daily placebo or NVP-BEZ235 administration and analyzed by immunostaining with specific antibodies against P-S6(Ser240/244), Ki67, and cleaved caspase-3 (cc3). Scale bars: 20 μ m (immunohistochemistry), 50 μ m (immunofluorescence). (C) Quantification of the immunostainings for P-S6 and cc3 and LI for Ki67 of the pituitary adenomas from 3 placebo-treated and 3 NVP-BEZ235-treated rats. **, P < 0.01.

Fig 3. DW-MRI to assess the response of rat pituitary adenomas to NVP-BEZ235. (A) T2-weighted MR images of the pituitary gland of a mutant rat treated with NVP-BEZ235 (treated, left) or with placebo (right) for 14 days (Top panels). Pseudo-colored apparent diffusion coefficient (ADC) maps of the same pituitary adenomas (Lower panels). The pituitary gland is marked in each image. (B) Size (top) and ADC values (bottom) of the pituitary adenomas before (pre) and after (post) 14 days of NVP-BEZ235 (treated, n=8) or placebo (n=4) administration. **, P=0.0013.

Fig 4. Expression of *Defb1*, *Tnfrsf10b*, *Bcl2a1* in rat pituitary adenoma tissues after NVP-BEZ235 treatment *in vivo*. RNA was extracted from microdissected pituitary adenomas after 14 days of treatment with placebo (n=4) or NVP-BEZ235 (n=4). qRT-PCR was performed using TaqMan primer and probe sets specific to rat *Defb1* (A), *Tnfrsf10b* (B), *Bcl2a1* (C). The relative mRNA expression level of the target genes was normalized for input RNA using rat β 2-microglobulin gene expression (housekeeping gene) and was calculated with the $2^{-\Delta\Delta Ct}$ formula. The obtained relative value was normalized against the average expression of placebo-treated tissues arbitrarily set to 1. Data were analyzed independently with six replicates each and are expressed as the mean \pm SEM. *, $P < 0.05$.

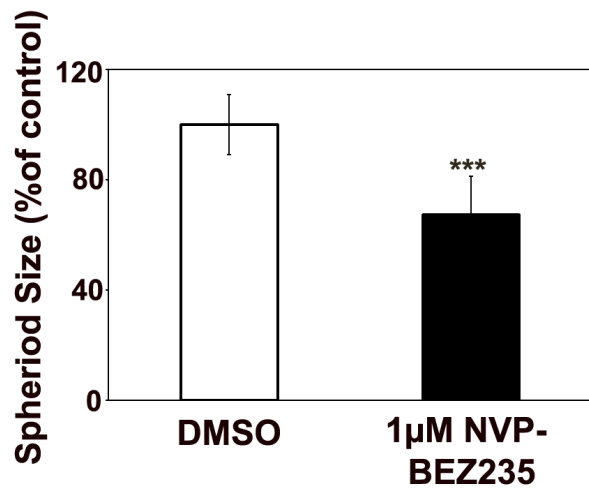
Fig 5. Expression of *DEFB1* in human NFPAs and immortalized gonadotroph cells. (A) RNA was extracted from frozen human normal pituitary (n=3) and NFPA samples (n=6). qRT-PCR was performed using TaqMan primer and probe sets specific to human *DEFB1*. The relative mRNA expression level of the target genes was normalized for input RNA using human *TBP* gene expression (housekeeping gene) and was calculated with the $2^{-\Delta\Delta Ct}$ formula. Data were analyzed independently with six replicates each and are expressed as the mean \pm SEM. *, $P < 0.05$. (B) Indirect immunofluorescence was performed using antibodies against BD-1 on human normal pituitary and NFPAs. Nuclei were counterstained with DAPI. For the adenomas, the tumor area is indicated (T). Scale bar: 50 μ m. (C) α T3 cells were treated with 1 μ M NVP-BEZ235 or DMSO and 24hrs later the level of *Defb1* was assessed by qRT-PCR. **, $P < 0.01$. (D) α T3 cells were plated on coverslips in 24-well plates and were incubated with 1 μ M NVP-BEZ235 or DMSO. Twenty-four hrs later cells were fixed, and processed for immunofluorescence with anti-BD-1 antibody. Nuclei were counterstained with DAPI. Scale bar: 50 μ m. (E) In samples parallel to C, proteins were extracted, and Western blotting was performed to monitor P-AKT (Ser473), total AKT, P-S6 (Ser240/244) and total S6. α -Tubulin was used as loading control.

Fig 6. Role of *Defb1* in NET cell lines. BON1 cells (A) and QGP1 cells (B) were treated with 1 μ M NVP-BEZ235 and 24hrs later the level of *DEFB1* was analyzed by qRT-PCR. In parallel, proteins were extracted, and Western blotting was performed to monitor P-AKT (Ser473), total AKT, P-S6 (Ser240/244) and total S6. α -Tubulin was used as loading control. (C) BON1 cells and QGP1 cells were plated on coverslips in 24-well plates and were incubated with 1 μ M NVP-BEZ235 or DMSO. Twenty-four hrs later cells were fixed, and processed for immunofluorescence with anti-BD-1 antibody.

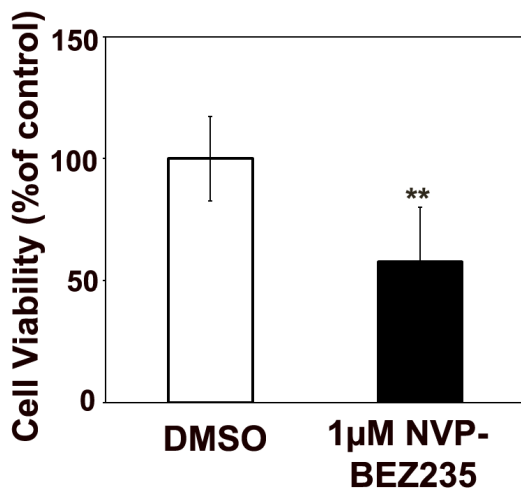
Nuclei were counterstained with DAPI. Scale bar: 50 μ m. BON1 cells (D) and QGP1 cells (F) were transfected with 20pmol of scrambled or anti-*DEFB1* siRNA pooled oligos and 24 hrs later treated with NVP-BEZ235 or DMSO. Cell proliferation was assessed after 24 hrs by measuring ATP levels. (E, G) In samples parallel to D and F, we monitored for caspase-3/7 activity. Data were analyzed independently with six replicates each and were expressed as the mean \pm SEM. *, P<0.05; **, P<0.005, *versus* scrambled.

Figure 1

A



B



C

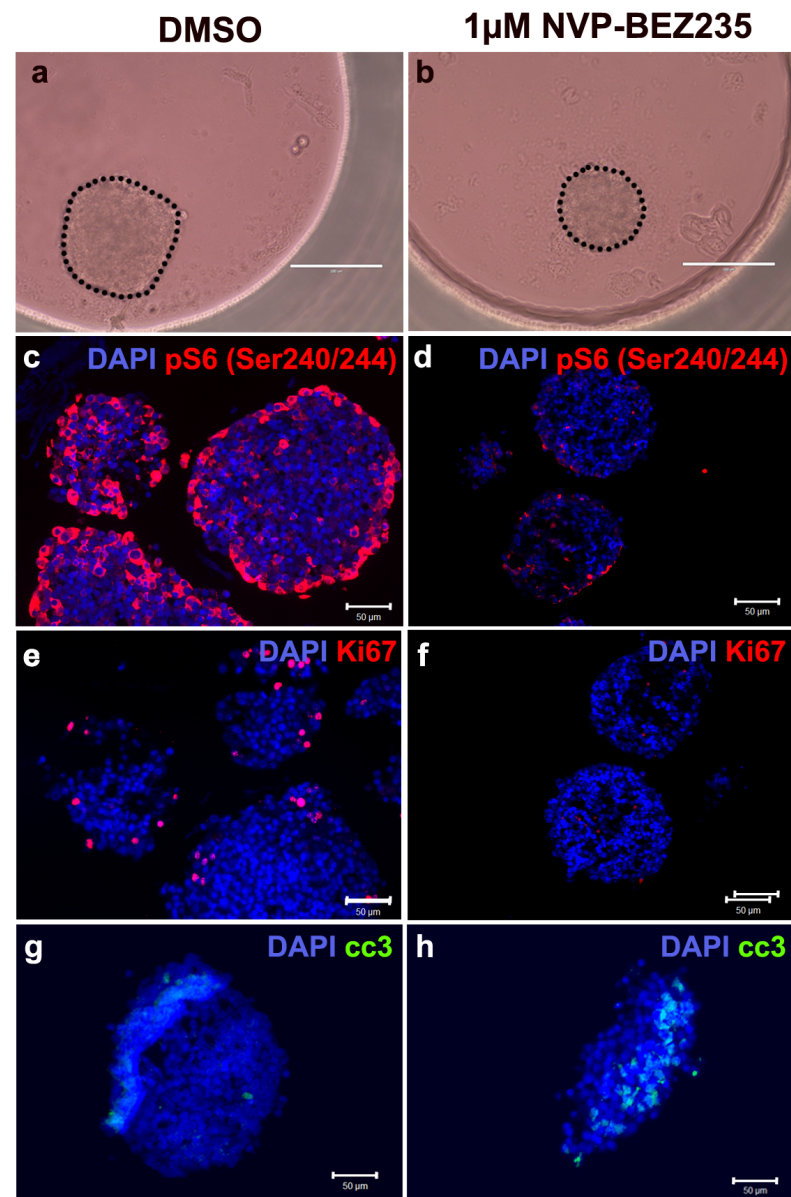
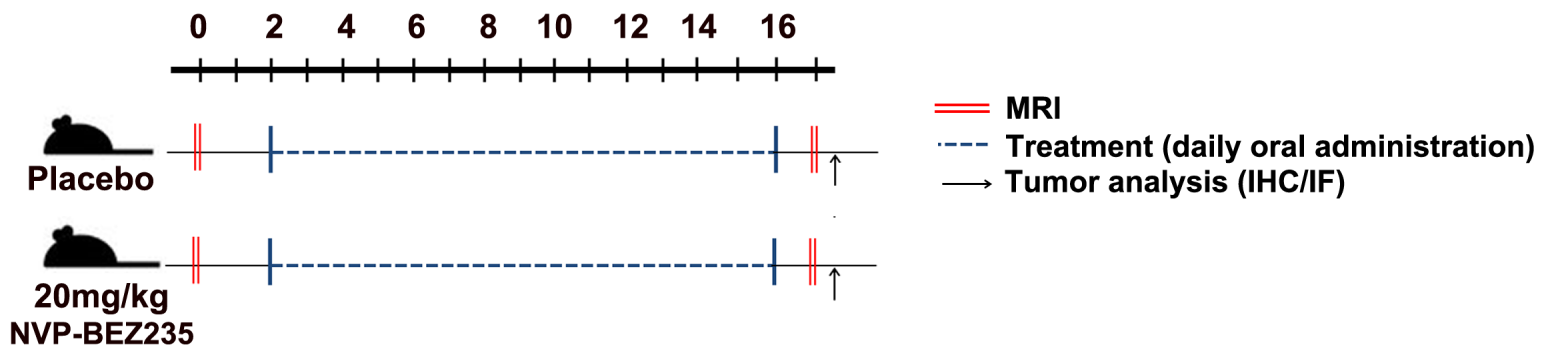
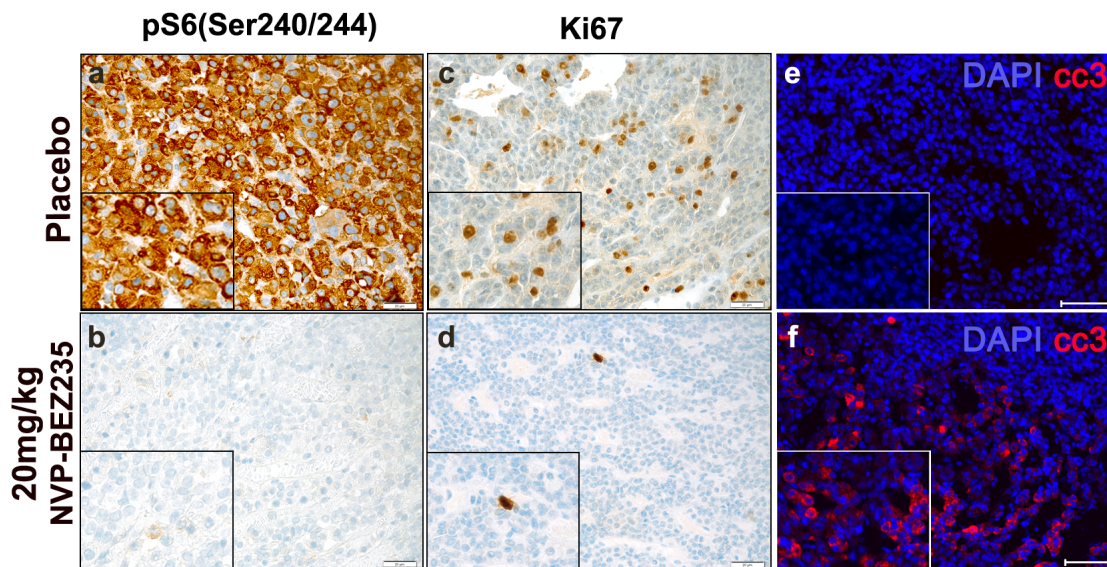


Figure 2

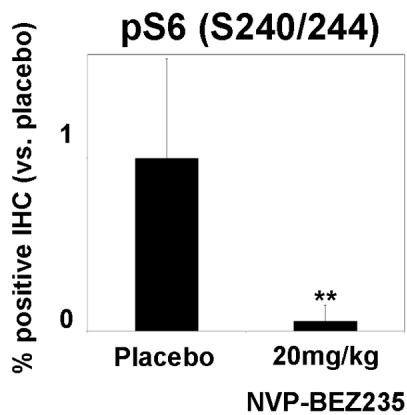
A



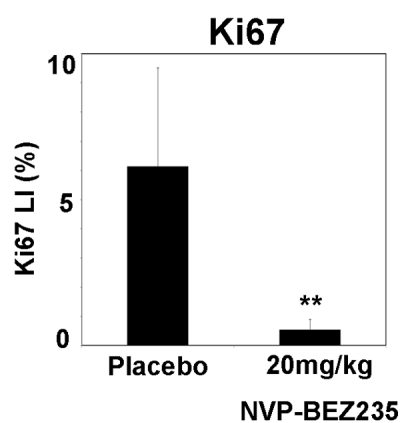
B



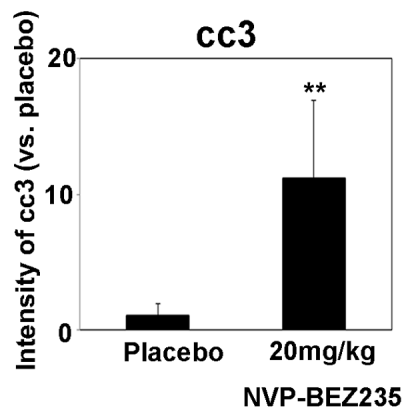
C



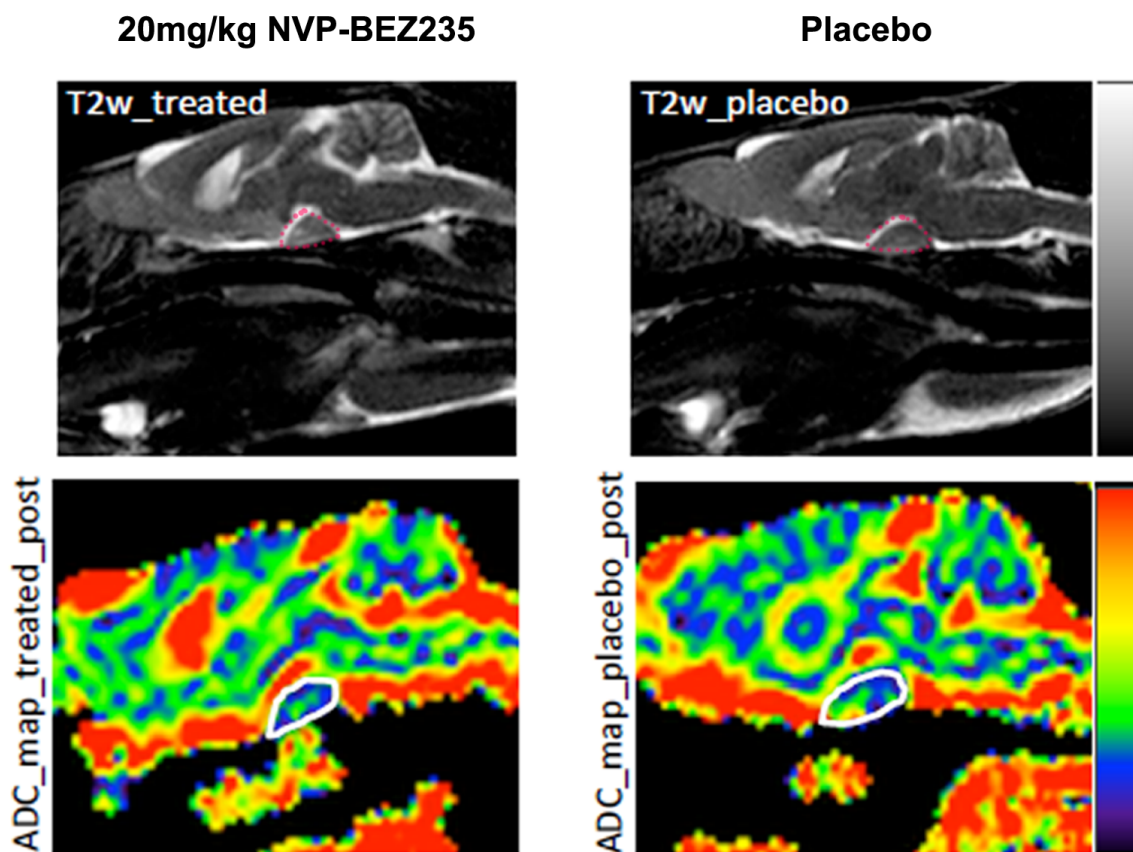
D



E



A



B

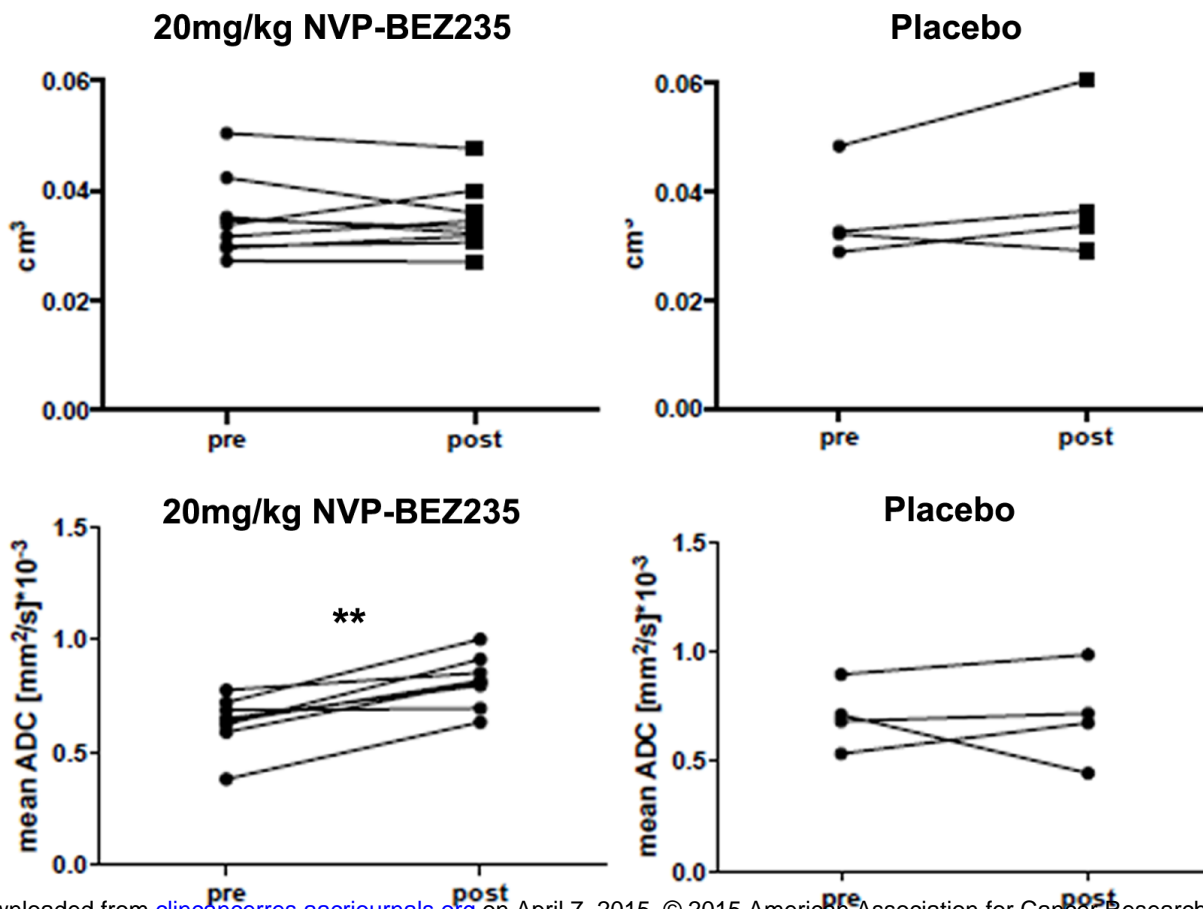
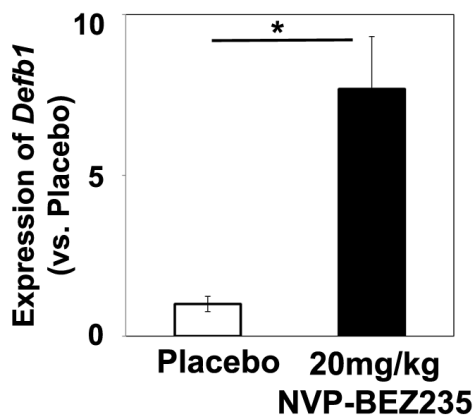
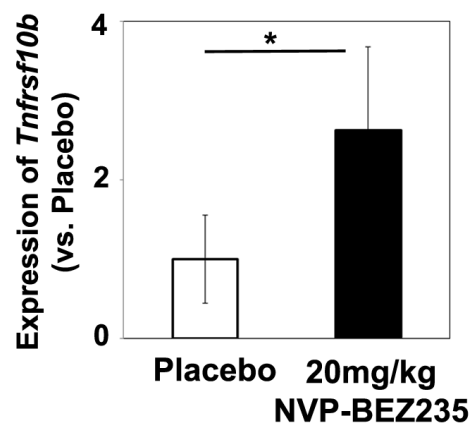


Figure 4

A



B



C

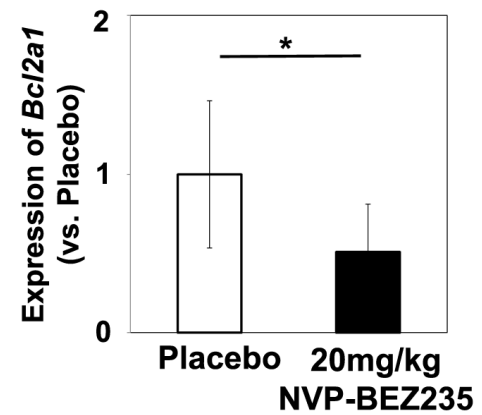
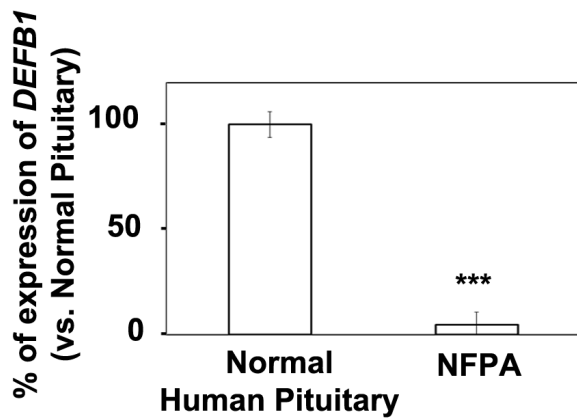
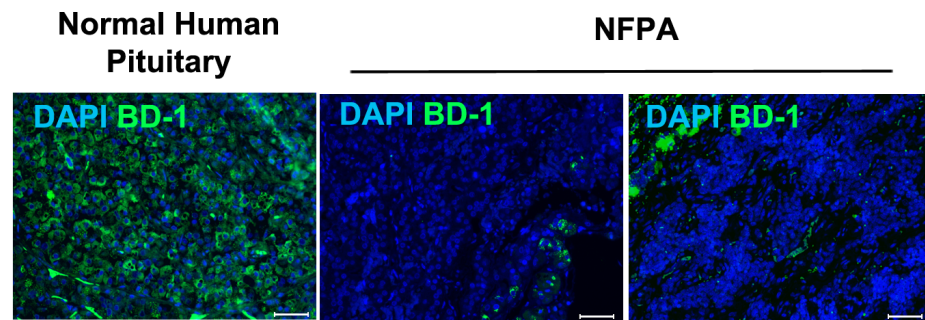


Figure 5

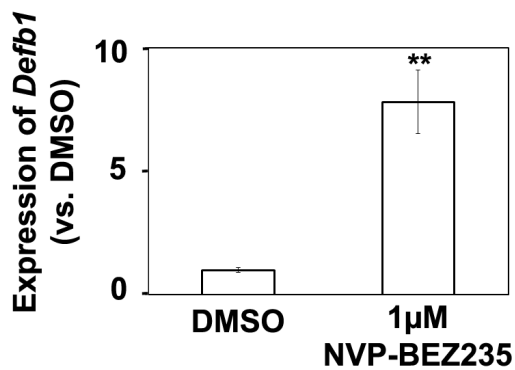
A



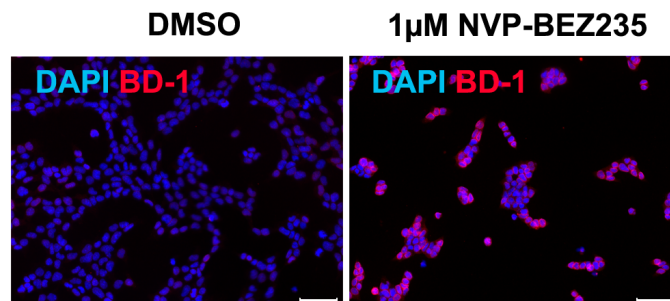
B



C



D



E

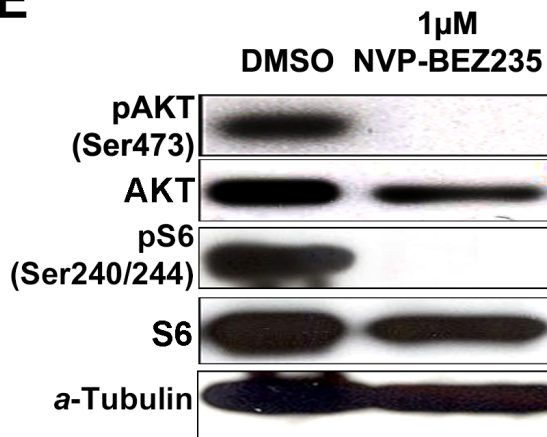
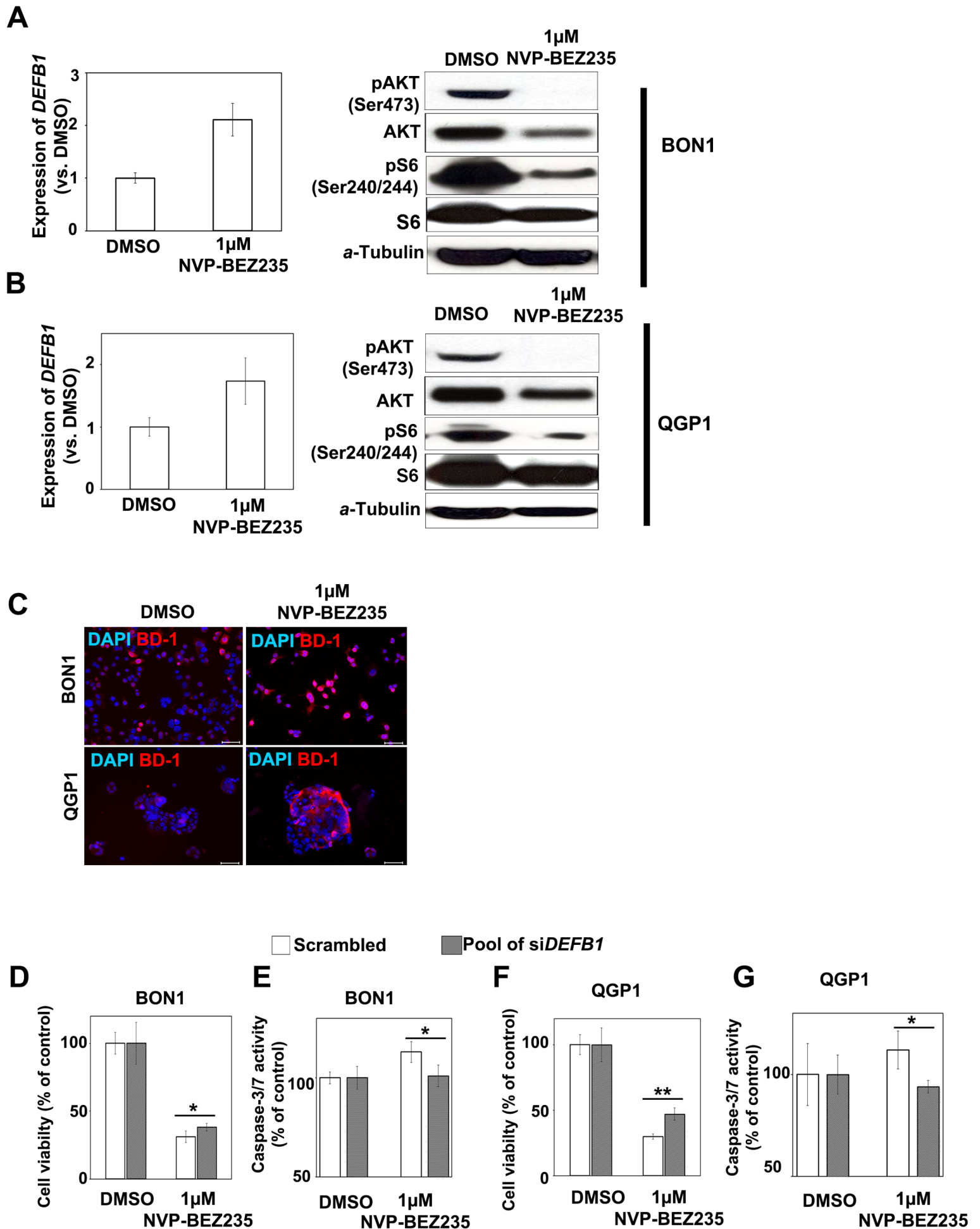


Figure 6



Clinical Cancer Research

Targeting PI3K/mTOR signaling displays potent antitumor efficacy against nonfunctioning pituitary adenomas

Misu Lee, Tobias Wiedemann, Claudia Gross, et al.

Clin Cancer Res Published OnlineFirst April 2, 2015.

Updated version	Access the most recent version of this article at: doi: 10.1158/1078-0432.CCR-15-0288
Supplementary Material	Access the most recent supplemental material at: http://clincancerres.aacrjournals.org/content/suppl/2015/04/04/1078-0432.CCR-15-0288.DC1.html
Author Manuscript	Author manuscripts have been peer reviewed and accepted for publication but have not yet been edited.

E-mail alerts	Sign up to receive free email-alerts related to this article or journal.
Reprints and Subscriptions	To order reprints of this article or to subscribe to the journal, contact the AACR Publications Department at pubs@aacr.org .
Permissions	To request permission to re-use all or part of this article, contact the AACR Publications Department at permissions@aacr.org .